PNAS
www.pnas.org

Supplementary Information for

Longitudinal Dynamics of the Human B Cell Response to the Yellow Fever 17D Vaccine

Anna Z. Wec[a], Denise Haslwanter[b], Yasmina N. Abdiche[c], Laila Shehata[a,†], Nuria Pedreño-Lopez[d], Crystal L. Moyer[e], Zachary A. Bornholdt[e], Asparouh Lilov[a], Juergen H. Nett[a], Rohit K. Jangra[b], Michael Brown[a], David I. Watkins[d], Clas Ahlm[f], Mattias N. Forsell[f], Félix A. Rey[g], Giovanna Barba-Spaeth[g], Kartik Chandran[b], Laura M. Walker[a,1]

Corresponding author: Laura M. Walker
Email: laura.walker@adimab.com

This PDF file includes:

> Supplementary text
> Figures S1 to S17
> Tables S1 to S2
> SI References

Materials and Methods

Cells. Huh 7.5.1 cells (received from Dr. Jan Carette; originally from Dr. Frank Chisari) were passaged every 3 to 4 days using a 0.05% Trypsin/EDTA solution (Gibco) and maintained in Dulbecco's Modified Eagle Medium (DMEM high glucose, Gibco) supplemented with 10% heat-inactivated fetal bovine serum (FBS, Atlanta Biologicals), 1% Penicillin/Streptomycin (P/S, Gibco), 1% Gluta-MAX (Gibco) and 25 mM HEPES (Gibco).

Vero African grivet monkey kidney cells (obtained from ATCC) were passaged every 3 to 4 days using 0.05% Trypsin/EDTA solution (Gibco) and maintained in Dulbecco's Modified Eagle Medium (DMEM high glucose, Gibco) supplemented with 2% heat-inactivated fetal bovine serum (FBS, Atlanta Biologicals), 1% P/S (Gibco), 1% Gluta-MAX (Gibco) and 25 mM HEPES (Gibco).

Yellow fever virus 17D generation. YFV-17D was obtained from BEI Resources (Cat# NR-115). 15 cm plates containing Huh 7.5.1 at a confluency of 80% were infected with 90 µl of a passage 2 stock of YFV-17D supernatant in 3 ml of infection media [DMEM low glucose (Gibco), 7% FBS (Atlanta Biologicals), 1% Pen-Strep (Gibco), 1% Gluta-MAX (Gibco), 25 mM HEPES (Gibco)] for 1 hr at 37 °C and 5% CO_2. After 3 days the supernatant was harvested and centrifuged twice at 4,000 rpm for 15 min at 4 °C to remove cell debris. The cleared viral supernatant was aliquoted, frozen at -80 °C and used for neutralization assays.

The YFV-17D viral stock used for ELISA was generated by ultracentrifugation of the pre-cleared supernatant at 28,000 rpm using a SW28 rotor (Beckman Coulter) in a Beckman Coulter Optima LE-80K ultracentrifuge for 4 h through a 2 ml cushion of 30% (v/v) D-sucrose/PBS. The pellet was allowed to resuspend overnight on ice in 300 µl PBS and was then aliquoted and frozen at -80 °C.

Zika virus generation. ZIKV strain MR 766 was obtained from ATCC (ATCC® VR-84™). For neutralization assays, 15 cm plates with Vero cells at a confluency of 80% were infected with 90 µl of a passage 1 stock of ZIKV supernatant in 3 ml of infection media [DMEM low glucose (Gibco), 2% FBS (Atlanta Biologicals), 1% Pen-Strep (Gibco), 1% Gluta-MAX (Gibco), 25 mM HEPES (Gibco)] for 1 h at 37 °C and 5% CO_2. After 3 days, the supernatant was harvested and centrifuged twice at 4,000 rpm for 15 min at 4 °C to remove cell debris. The cleared viral supernatant was aliquoted, frozen at -80 °C and used for neutralization assays.

WNV and JEV reporter particle generation.

West Nile virus (WNV) subgenomic replicon-expressing plasmid pcDNA6.2-WNIIrep-GFP/zeo and WNV structural protein expression plasmid pcDNA6.2-WNI-CPrME (Strain NY99) were a generous gift from Ted Pierson (PMID: 16325883). The structural proteins C, prM and E of the Japanese encephalitis virus (JEV, strain AT31; GenBank BAD81039.1) were synthesized and codon-optimized for expression in human cells by Epoch Life Science, Inc into the pCAGGS vector. To produce RVPs, 293FT cells (Thermo

Fisher) were transfected with 12 µg of total DNA per plate in a ratio of 1:3 using the WNV replicon plasmid and the respective flavivrus CprME plasmid. Eight hours after transfection, media was changed to low glucose DMEM (Gibco) media containing 5% FBS (Atlanta Biologicals) and 25 mM HEPES (Gibco). After 3 days at 37 °C under 5% CO_2, the cell supernatant containing RVPs was harvested and centrifuged twice for 15 min at 4,000 rpm at 4°C to remove the cell debris. The viral supernatant was pelleted using a SW28 rotor (Beckman Coulter) in a Beckman Coulter Optima LE-80K ultracentrifuge for 4 hrs through a 2 ml cushion of 30% (v/v) D-sucrose in PBS, (pH 7.4). The pellet was resuspended overnight on ice in 150 µl PBS (pH 7.4), aliquoted and stored at -80 °C.

Production of recombinant YFV antigens. The coding region for the entire prM and soluble E (sE) region of the YFV Asibi Strain (Uniprot ID: Q6DV88, residues 122-678 of the genome polyprotein) was cloned into pMT-puro, an insect expression vector encoding a C-terminal double strep tag**.** Expression construct design was based on previously published structures of flavivirus antigens(1-3). The YFV prM/E construct was used to generate an inducible, stable Drosophila S2 line. Protein expression was induced with addition of copper sulfate and allowed to proceed for 5–7 days. Recombinant protein was affinity-purified from the culture supernatant with a StrepTrap HP column (GE Healthcare). An additional purification step was carried out using size-exclusion chromatography step using an S200Increase column (GE Healthcare). The final protein preparations were stored in phosphate-buffered saline (pH 7.4) supplemented with an additional 150 mM NaCl. Small aliquots were stored at -70 ˚C until use.

Flavivirus NS1 protein antigens. The NS1 proteins from DENV1-4, JEV, TBEV, WNV, YFV were purchased from the Native Antigen Company (Cat# FLAVX4-NS1-100 and DENVX4-NS1-100) and the ZIKV NS1 was purchased from Meridian Life Science (Cat# R01636). The positive control anti-NS1 antibodies were obtained from the Native Antigen Company (anti-DENV NS1, Cat# AbDENVNS1-DA034; anti-ZIKV NS1, Cat# AbZIKVNS1-B4-100). The anti-YFV NS1 protein antibody was purchased from Meridain Life Sciences (Cat# C01906M). The anti-WNV NS1 antibody (Cat# HM484-X0632) and anti-TBEV NS1 antibody (Cat# HM477-X1462) were purchased from East Coast Bio. Flavivirus cross-reactive serum was used to detect the JEV NS1 protein.

YFV-17D DIII protein. The DIII region (aa 293-397) of the YFV-17D E protein (Uniprot ID: P03314) was produced in Drosophila S2 cells using a modified pT350 vector (Felix Rey, Institut Pasteur, France. Protein expression was induced by $CdCl_2$ and the supernatant was harvested 5 - 7days post-induction. Recombinant protein was purified using a Strep-Tactin column (IBA) and size-exclusion chromatography using a S200Increase column (GE Healthcare) and 10 mM Tris (pH 8)/150 mM NaCl buffer.

Single B cell sorting. For plasmablast sorting, PBMCs were stained using anti-human CD38 (PE; Biolegend Cat# 356604), CD27 (BV421; BD Bioscience Cat# 562513), CD19 (PE-Cy7; Biolegend Cat# 302312), CD20 (APC-Cy7; Biolegend Cat# 302218), CD3 (PerCP-Cy5.5; Biolegend Cat# 300430), CD8 (PerCP-Cy5.5; Biolegend Cat# 344710), CD14 (PerCP-Cy5.5; Invitrogen Cat# 45-0149-42) and CD16 (PerCP-Cy5.5; Biolegend Cat# 360712). Plasmablasts were defined as

3

CD19$^+$CD3$^-$CD20$^{-/lo}$CD27^{high}CD38^{high} cells. For MBC sorting, B cells were purified using a MACS B cell isolation kit (Miltenyi Biotec; Cat# 130-091-151) and subsequently stained using anti-human CD19 (PE-Cy7; Biolegend Cat# 302312), CD20 (PE-Cy7; Biolegend Cat# 302312), CD3 (PerCP-Cy5.5; Biolegend Cat# 300430), CD8 (PerCP-Cy5.5; Biolegend Cat# 344710), CD14 (PerCP-Cy5.5; Invitrogen Cat# 45-0149-42), CD16 (PerCP-Cy5.5; Biolegend Cat# 360712), IgD (BV421; Biolegend Cat# 348226), IgM (AF-488; Biolegend Cat# 314534), CD27 (BV510; BD Biosciences Cat# 740167), CD21 (BV605; BD Biosciences Cat# 740395), CD71 (APC-Cy7; Biolegend Cat# 334110) and a mixture of APC- and PE-labeled YFV E tetramers (25 nM each). Tetramers were prepared fresh for each experiment using Streptavidin-PE (Life Technologies Cat# S21388) and Streptavidin-APC (Life Technologies Cat#32362). B cells that showed reactivity to the YFV E tetramers were single cell sorted using a BD FACS Aria Fusion (BD Biosciences) into 96-well PCR plates (Bio-Rad) containing 20 µl /well of lysis buffer [5 µl of 5X first strand cDNA buffer (Invitrogen), 0.625 µl of NP-40 (New England Biolabs), 0.25 µl RNaseOUT (Invitrogen), 1.25 µl dithiothreitol (Invitrogen), and 12.6 µl dH$_2$O]. Plates were immediately stored at -80 ˚C. Flow cytometry data was analyzed using FlowJo software.

Amplification and cloning of antibody variable genes. Antibody variable genes (IgH, IgK, and IgL) were amplified by reverse transcription PCR and nested PCRs using cocktails of IgG-, IgD-, IgA-, and IgM-specific primers, as described previously(4). The primers used in the second round of PCR contained 40 base pairs of 5' and 3' homology to the digested expression vectors, which allowed for cloning by homologous recombination into *S. cerevisiae*. Yeast were transformed using the lithium acetate method for chemical transformation(5). Approximately 10 µl of unpurified V$_H$ and V$_L$ PCR product and 200 ng of the digested expression vectors were used for each transformation reaction. Following transformation, individual yeast colonies were picked for sequencing.

Expression and purification of IgGs. IgGs were expressed in *S. cerevisiae* cultures grown in 24-well plates, as described previously(6). After 6 days, the cultures were harvested by centrifugation and IgGs were purified by protein A-affinity chromatography. The bound antibodies were eluted with 200 mM acetic acid/50 mM NaCl (pH 3.5) into 1/8th volume 2 M Hepes (pH 8.0) and buffer-exchanged into PBS (pH 7.0).

Fab fragments were generated by digesting the IgGs with papain for 2 hrs at 30 °C. The digestion was terminated by the addition of iodoacetamide, and the Fab and Fc mixtures were passed over Protein A agarose to remove Fc fragments and undigested IgG. The flow-through of the Protein A resin was then passed over CaptureSelect™ IgG-CH1 affinity resin (Thermo Fisher Scientific) and eluted with 200 mM acetic acid/50 mM NaCl (pH 3.5) into 1/8th volume 2 M Hepes (pH 8.0). Fab fragments then were buffer exchanged into PBS (pH 7.0).

Surface plasmon resonance kinetic measurements of IgG binding. A Biacore 8K system docked with a CAP sensor chip sample compartment was set to 10 °C, flow cell temperature to 25 °C, and the data collection rate to 10 Hz. HBS-EP+ [10 mM HEPES (pH 7.3), 150 mM NaCl, 3 mM EDTA, 0.05%

4

Surfactant P20] was used as the running buffer. In each cycle, biotin CAPture reagent (GE Healthcare) diluted 1:20 in running buffer was injected over flow cells 1 and 2 for 600 s, at a flow rate of 5 µl /min, followed by a 900 s capture (1 µl /min) of biotinylated YFV E antigen (25 nM in HBS-EP+) over flow cell 2 to reach a minimum capture level of 400 RU. The IgGs (36 – 288 nM in HBS-EP+) were then injected over flow cells 1 and 2 for 300 s (30 µl /min), the dissociation monitored for 300 s (30 µl /min), and the surface regenerated at the oligonucleotide level with 6M Guanidine-HCl in 0.25 M NaOH for 120 s (10 µl /min). A minimum of two blank (HBS-EP+) injections also were run under identical conditions as described above and used to assess and subtract system artifacts. The data were aligned, double referenced, and fit to a bivalent analyte binding model using Biacore 8K Evaluation Software, version 1.0.

Bio-Layer Interferometry Kinetic Measurements (BLI). For monovalent apparent K_D determination, IgG binding to recombinant YFV E antigen was measured by biolayer interferometry (BLI) using a FortéBio Octet HTX instrument (Molecular Devices). The IgGs were captured (1.5 nm) to anti-human IgG capture (AHC) biosensors Molecular Devices) and allowed to stand in PBSF (PBS with 0.1% w/v BSA) for a minimum of 30 min. After a short (60 s) baseline step in PBSF, the IgG-loaded biosensor tips were exposed (180 s, 1000 rpm of orbital shaking) to YFV E antigen (100 nM in PBSF) and then dipped (180 s, 1000 rpm of orbital shaking) into PBSF to measure any dissociation of the antigen from the biosensor tip surface. Data for which binding responses were > 0.1 nm were aligned, inter-step corrected (to the association step) and fit to a 1:1 binding model using the FortéBio Data Analysis Software, version 11.1.

For bivalent apparent K_D determination, IgG binding to recombinant biotinylated YFV E antigen was measured by BLI using a FortéBio Octet HTX instrument (Molecular Devices). Recombinant biotinylated YFV E was immobilized on streptavidin biosensors (Molecular Devices) and allowed to stand in PBSF (PBS with 0.1% w/v BSA) for a minimum of 30 min. After a short (60 s) baseline step in PBSF, the antigen-loaded biosensor tips were exposed (180 s, 1000 rpm of orbital shaking) to the IgGs (100 nM in PBSF) and then dipped (180 s, 1000 rpm of orbital shaking) into PBSF to measure any dissociation of the IgGs from the biosensor tip surface. Data for which binding responses were > 0.1 nm were aligned, interstep corrected (to the association step) and fit to a 1:1 binding model using the FortéBio Data Analysis Software, version 11.1.

Bio-Layer Interferometry (BLI) Epitope Binning. Control antibodies 5A and 4G2 (produced as human IgG1 chimeras) were captured on anti-human IgG capture biosensors (0.9 nm) (Molecular Devices) and the biosensors were then blocked by exposing them to adalimumab (0.5 mg/ml; 20 min, 350 rpm of orbital shaking). After a short (60 s) baseline step in PBSF, a cross-interaction check was performed between the sample IgGs and the loaded biosensors (180 s, 1000 rpm of orbital shaking). No cross-interaction was observed for this panel of IgGs. The loaded biosensors were then subjected to a second short (60 s) baseline step in PBSF, followed by an association step in 100 nM recombinant YFV E monomer (180 s, 1000 rpm of orbital shaking). Finally, the binning step was performed in 100 nM sample IgGs in PBS with 0.1% BSA (PBSF) (180 s, 1000 rpm of orbital shaking). Data were analyzed using the FortéBio Data

Analysis Software, version 11.1. Sample IgGs with a binning response lower than 0.1 nm were determined to compete with the control antibody. Sample IgGs with a binning response greater than 0.1 nm were determined to be non-competitors to the control antibody.

High-throughput epitope binning using Carterra LSA. Carterra's LSA was used to perform epitope binning assays in a classical sandwich assay format(7) using five benchmark mAbs (ADI-44112, ADI-45107, ADI-49147, 4G2, and 5A) as analytes. An HCX-30M (pre-activated) chip type was used and experiments were performed at 25 ºC. The SFC and 96PH were primed in run buffer of 25 mM Mes (pH 5.5) + 0.01% Tween20. The test mAbs were diluted to 2 µg/ml in 10 mM sodium acetate (pH 4.5; coupling buffer) and coupled via the 96PH using 7 min contact time at each print block location. After 4 serial docks of the 96PH to build up a 384-ligand array, the SFC was docked over the entire surface to quench excess reactive esters by injecting ethanolamine (pH 8.5) for 7 min. Final coupled levels of each mAb ranged from 1000-4000 RU per spot. The 96PH was returned to water for cleaning and the SFC was primed in an assay run buffer of HBSET + 0.5 g/l BSA. Each binning cycle involved a co-inject style of sample delivery whereby the antigen (50 nM YFV E) and antibody analyte (20 µg/ml mAb or buffer) samples were injected back-to-back, with minimal dissociation time between them over the 384-ligand array. Typical association times were 3 or 5 mins and surfaces were regenerated with 75 mM phosphoric acid after each binning cycle. The binding data were analyzed using Carterra's Epitope Software.

Serum and purified IgG ELISAs. For NS1 and E binding ELISAs, 96-well plates (Corning) were coated with 5 µg/ml of NS1 or E protein diluted in PBS and incubated overnight at 4 °C. Wells were washed and then blocked with 5% non-fat dried milk (NFDM) in PBS for 1 hr at 37 °C. Wells were washed three times with PBS and serial dilutions of human plasm in 5% NFDM-PBS were added and incubated for 1 hr at 37 °C. Plates were then washed three times with PBS and secondary cross-adsorbed anti-human IgG-HRP (Thermo Fisher Scientific) or anti-human-IgM (Sigma Aldrich) detection antibodies were added at 1:8000 dilution in 5% NFDM-PBS for 1 h at 37 °C. After washing three times with PBS, the 1-Step™ Ultra TMB-ELISA Substrate Solution (Thermo Fisher Scientific) was added to detect binding as per manufacturer recommendations (Thermo Fisher Scientific) and absorbance was measured at 450 nm wavelength using a Spectramax microplate Reader (Molecular Devices).

For virus binding ELISAs, 96-well ELISA plates were coated with 5 µg/ml of 4G2 (Millipore, Cat# MAB10216) diluted in phosphate buffered saline (PBS) and incubated for 2 hrs at 37 °C. After washing three times with PBS, whole YFV-17D viral particles diluted in PBS (pH 7.4) were added to the wells and incubated overnight at 4 °C. Plates were then washed three times with PBS and blocked with 5% non-fat dried milk in PBS (NFDM-PBS) for 1 hr at 37 °C. After removal of the blocking solution, test antibodies diluted in 5% NFDM-PBS to 100 nM were allowed to bind for 1 hr at 37 °C. Plates were then washed three times with PBS and secondary cross-adsorbed anti-human IgG-HRP (Thermo Fisher Scientific; Cat# 31413) or anti-human-IgM (Sigma Aldrich; Cat# AP114P) detection antibodies were added at 1:8000 dilution in 5% NFDM-PBS for 1 hr at 37 °C. After washing three times with PBS, the 1-Step™

Ultra TMB-ELISA Substrate Solution was added to detect binding as per manufacturer recommendations (Thermo Scientific; Cat# 34029) and absorbance was measured at 450 nm wavelength using a Spectramax microplate Reader (Molecular Devices).

Micro-titer neutralization assays. Monoclonal antibodies were serially diluted in DMEM high glucose medium (Gibco), supplemented with 10% heat-inactivated FBS (Gibco), 1% Gluta-MAX (Gibco), 1% P/S (Gibco) and 25 mM HEPES (Gibco), and incubated at room temperature with the test viruses (YFV-17D or ZIKV) or test RVPs (WNV or JEV) for 1 hr. YFV-17D and ZIKV were diluted to achieve 60% endpoint infection and the WNV and JEV RVPs to an endpoint infection of 10%. The antibody-virus mixture was added in triplicate to 96-well plates (Costar, Cat# 3595) containing $5x10^3$ Huh 7.5.1 cell monolayers seeded the day before. Cells were incubated for 2 days at 37 °C and 5% CO_2. Cells were then fixed with 4% paraformaldehyde (Sigma) for 10 min and subsequently washed with a Tris buffer [50 mM Tris, 150 mM NaCl (pH 7.6)], three times. Fixed cells were incubated with the pan-flavivirus mouse mAb 4G2 at 2 µg/ml in Tris buffer containing 3% nonfat dry milk powder (BioRad), 0.5% Triton X-100 (MP Biomedicals), and 0.05% Tween 20 (Fisher Scientific) for 1 hr at room temperature (RT). Afterwards, cells were washed three times and incubated with a goat anti-mouse secondary antibody conjugated to Alexa Fluor 488 (Invitrogen Cat# A-11029) at a 1:500 dilution for 1 hr at 25 °C. Cells were washed again and nuclei were stained with Hoechst-33342 (Life Technologies Cat# H3570) in a 1:2,000 dilution in PBS. Viral infectivity was measured by automated enumeration of Alexa Fluor 488-positive or GFP-positive cells from captured images using a Cytation-5 automated fluorescence microscope (BioTek) and analyzed using the Gen5 data analysis software (BioTek). The IC_{50}s of the mAbs were calculated using a nonlinear regression analysis with GraphPad Prism software. Viral neutralization data were subjected to nonlinear regression analysis to extract the values (GraphPad Prism).

Neutralization of donor plasma samples was carried out as described above for purified IgGs. Serial dilutions of plasma were pre-incubated with YFV-17D infectious stock for 1 hr before adding to cell monolayers. Purified total human IgG from non-immunized donors was used as negative control in purified IgG neutralization assays against YFV-17D and ZIKV (Jackson Immuno Research, Cat# AB_2337042).

FRNT assay. Virus-specific mAbs were screened as previously described(8). Briefly, purified mAbs were serially diluted in 199 medium (Thermo Scientific) containing 5% heat-inactivated fetal bovine serum (FBS; Gibco-Invitrogen) and incubated at 37 °C with YFV-17D. After a 1 hr incubation, the antibody-virus mixture was added in duplicate to 96-well plates containing 80% confluent monolayers of Vero E6 cells. Plates were incubated for 1.5 hrs at 37 °C. Wells were then overlaid with 1% methylcellulose in supplemented OptiMEM GlutaMAX media (Invitrogen) with 5% heat-inactivated FBS (Gibco-Invitrogen) and 1% amphotericin B and incubated at 37 °C, 5% CO_2 for 72 hrs. Cells were then fixed and permeabilized with Perm/Wash buffer (BD Biosciences) for 30 min. After permeabilization, cells were washed with PBS and incubated with a 1:2000 dilution of anti-flavivirus antibody (EMD Millipore, Cat#

MAB10216) in Perm/Wash buffer for 2 hrs. After incubation, cells were washed with PBS and incubated with anti-mouse horseradish peroxidase (HRP)–conjugated secondary antibody (Jackson ImmunoResearch Laboratories; Cat# 115035146) for 2 hrs. Plates were washed and developed with peroxidase substrate (KPL). The half maximal inhibitory concentration (IC$_{50}$) of the mAbs was calculated using a nonlinear regression analysis with GraphPad Prism software.

Polyreactivity assays. Polyreactivity was assessed using a previously described assay(9). Briefly, soluble membrane protein (SMP) and soluble cytosolic protein (SCP) fractions were prepared from Chinese hamster ovary cells and biotinylated with NHS-LC-Biotin reagent (Thermo Fisher Scientific). Two million IgG-presenting yeast were transferred to a 96-well assay plate and pelleted to remove the supernatant. The yeast pellets were resuspended in a 1:10 diluted stock of biotinylated SCPs and SMPs and incubated on ice for 20 min. Cells were washed twice with ice-cold PBSF, and the samples were incubated in 50 µl of secondary labeling mix (Extravadin-R-PE, goat F(ab') 2-anti human LC-FITC, and propidium iodide) on ice for 20 min. The samples were analyzed for both IgG expression (LC-FITC) and polyspecificity reagent (PSR)-binding using a FACS Canto II (BD Biosciences) with an HTS sample injector. Mean fluorescence intensity (MFI) values of each were recorded and the PSR binding value normalized as previously described(9).
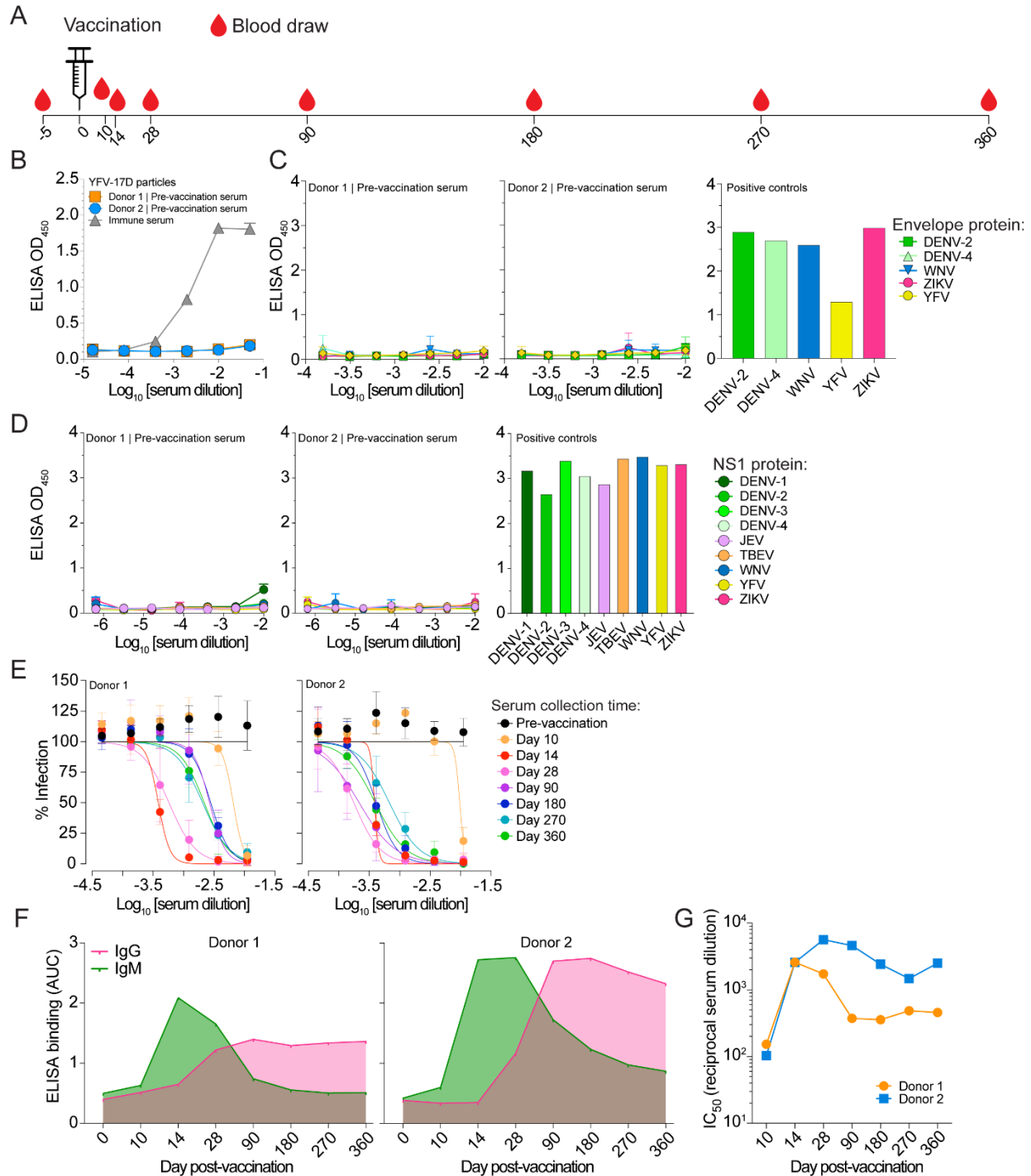
Fig. S1. YFV-17D immunization, blood draws and serum analysis. (A) Blood samples were collected five days before vaccination and on days 10, 14, 28, 90, 180, 270, and 360 following vaccination. **(B)** ELISA binding reactivity of pre-vaccination serum samples to YFV-17D particles immobilized on ELISA plates with murine 4G2. Binding of immune serum from a YFV-17D vaccinated donor is shown as a positive control. **(C)** ELISA binding reactivity of pre-vaccination serum samples against DENV-2, DENV-4, WNV-, and ZIKV-E proteins. Serum reactivity to JEV and TBEV E proteins was not tested due to lack of reagent availability. DENV and ZIKV immune serum was used as a positive control(12). **(D)** ELISA binding reactivity of pre-vaccination serum samples against ZIKV-, DENV1-4-, WNV-, JEV-, TBEV- and

9

YFV-NS1 proteins. A panel of positive control mAbs with specificity for ZIKV-, DENV1-4-, WNV-, JEV-, YFV-, and TBEV-NS1 proteins were tested at a 2 µg/ml concentration. **(E)** Serum neutralizing activity against YFV-17D at days -5 (pre-vaccination), 10, 14, 28, 90, 180, 270, and 360 post-vaccination. Averages ± SD (n = 6) from two independent experiments are shown. **(F)** Serum IgM and IgG binding kinetics following YFV-17D vaccination. Binding reactivity to YFV-17D particles immobilized with murine 4G2 was assessed by ELISA. **(G)** Neutralization IC_{50}s of serum samples at each time point post vaccination, expressed as reciprocal serum dilution. AUC; area under the curve.
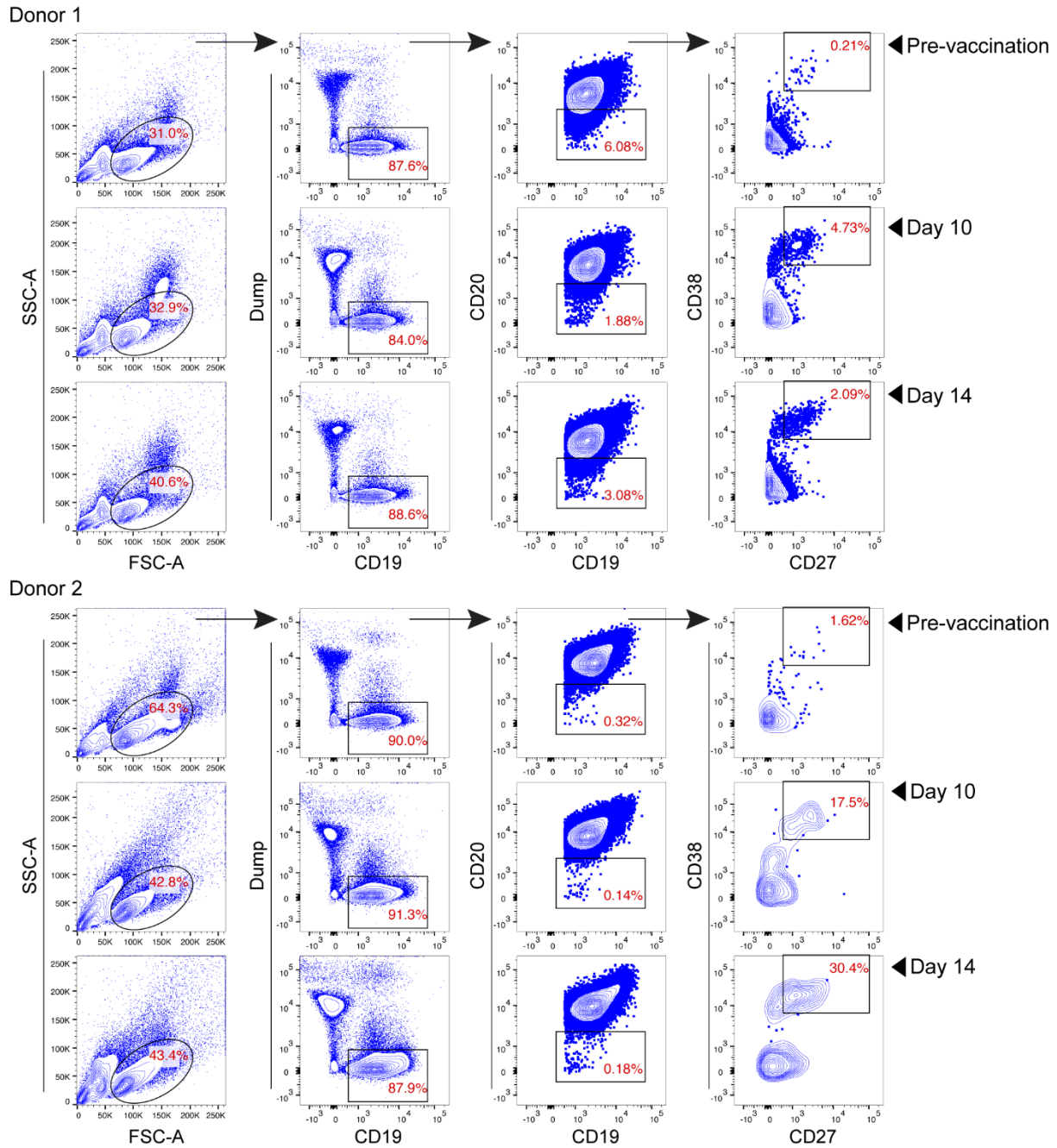
Fig. S2. Plasmablast sorting. PB responses were analyzed at days 10 and 14 following vaccination. Lymphocytes were gated based on forward- and side-scatter, followed by selection of PI⁻CD3⁻CD8⁻CD14⁻ cells. B cells were identified by gating on CD19⁺ cells. Plasmablasts, defined as CD19⁺CD20⁻/loCD38hiCD27hi cells, were single-cell sorted for mAb cloning. SSC-A, side scatter area; FSC-A, forward scatter area; PI, propidium iodide.
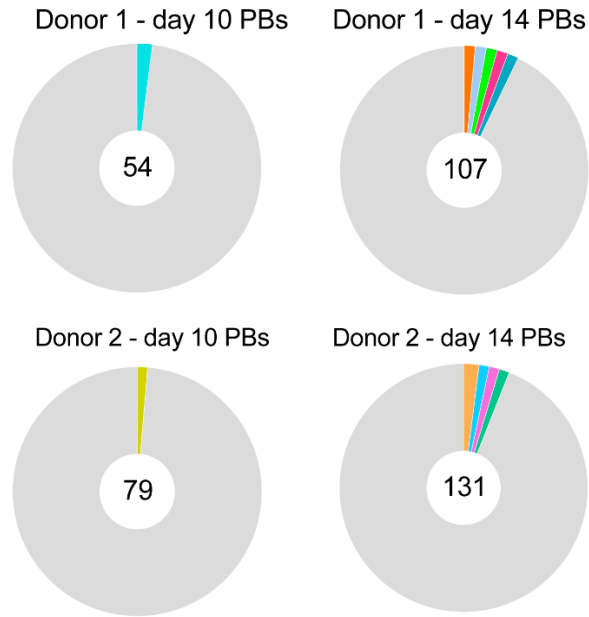
Fig. S3. Plasmablast clonal lineage analysis. Each lineage is represented as a segment proportional to the lineage size. All lineages that contain only a single sequence are combined and shown as a single grey segment. The total number of PB-derived mAbs is shown in the center of each pie. Clonal lineages were defined based on the following criteria: identical V_H and V_L germline gene, identical CDR H3 length, and CDR H3 amino acid identity ≥80%.
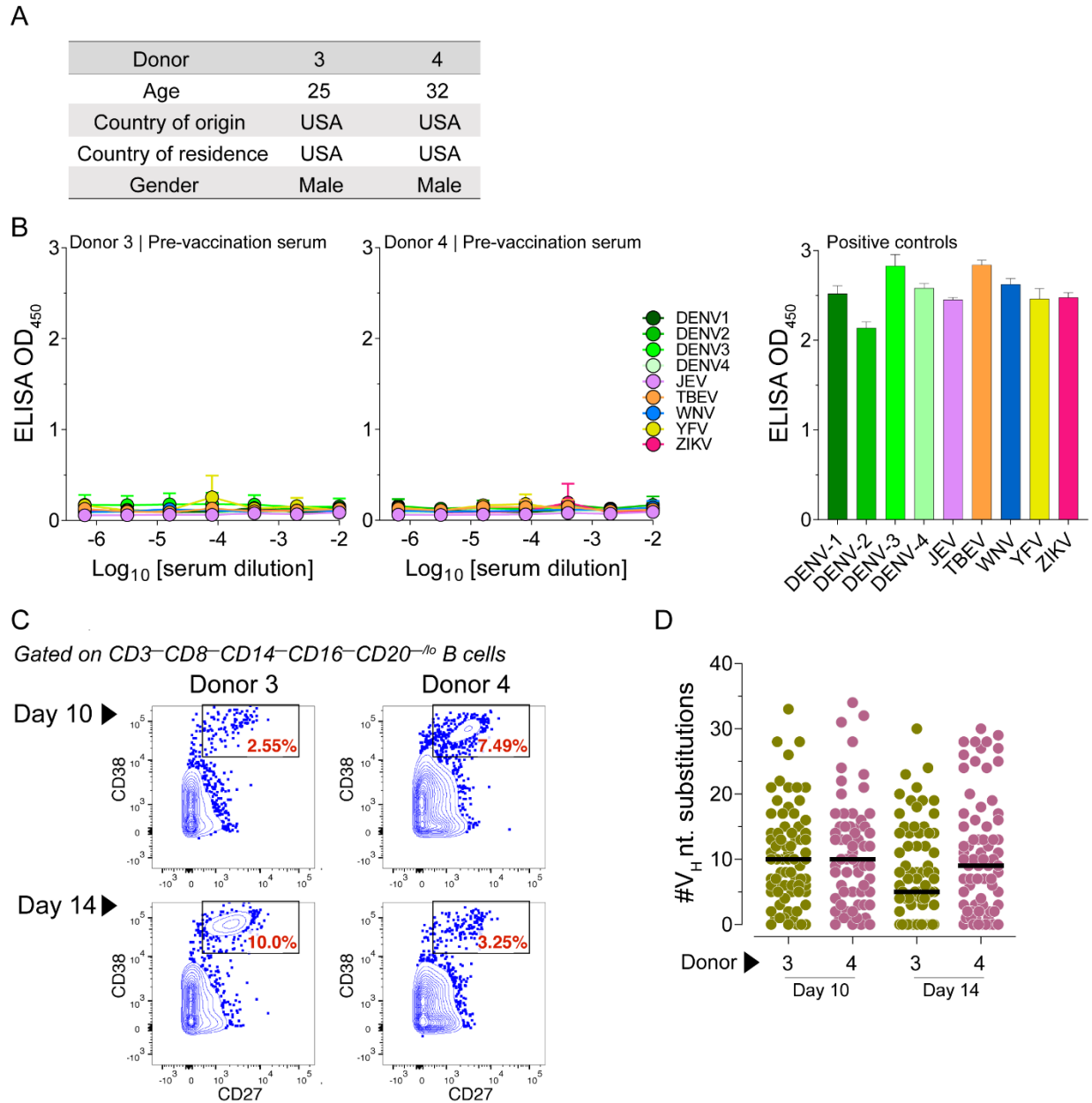
A

Donor	3	4
Age	25	32
Country of origin	USA	USA
Country of residence	USA	USA
Gender	Male	Male

B Donor 3 | Pre-vaccination serum — Donor 4 | Pre-vaccination serum — Positive controls

Legend: DENV1, DENV2, DENV3, DENV4, JEV, TBEV, WNV, YFV, ZIKV

ELISA OD$_{450}$ vs Log$_{10}$ [serum dilution]

Positive controls: DENV-1, DENV-2, DENV-3, DENV-4, JEV, TBEV, WNV, YFV, ZIKV

C

Gated on CD3⁻CD8⁻CD14⁻CD16⁻CD20⁻/lo B cells

Donor 3 — Donor 4

Day 10: Donor 3 = 2.55%, Donor 4 = 7.49%

Day 14: Donor 3 = 10.0%, Donor 4 = 3.25%

(CD38 vs CD27)

D

#V$_H$ nt. substitutions

Donor	3	4	3	4
	Day 10		Day 14	

Fig. S4. Characterization of PB responses in two additional YFV-17D vaccinated donors. (A) ELISA binding reactivity of pre-vaccination serum samples against ZIKV-, DENV1-4-, WNV-, JEV-, TBEV and YFV-NS1 proteins. A panel of positive control mAbs with specificity for ZIKV-, DENV1-4-, WNV-, JEV-, YFV-, and TBEV-NS1 proteins were tested at a 2 µg/ml concentration. (B) Flow cytometric analysis of PB responses on days 10 and 14 following vaccination. Plasmablasts, defined as CD19⁺CD20⁻/**lo**CD38^hiCD27^hi cells, were single-cell sorted for mAb sequencing. (C) SHM loads, expressed as number of nucleotide substitutions in V$_H$, of mAbs isolated from day 10 and day 14 PBs. Black bars indicate medians. nt, nucleotide; V$_H$, variable region of the heavy chain.
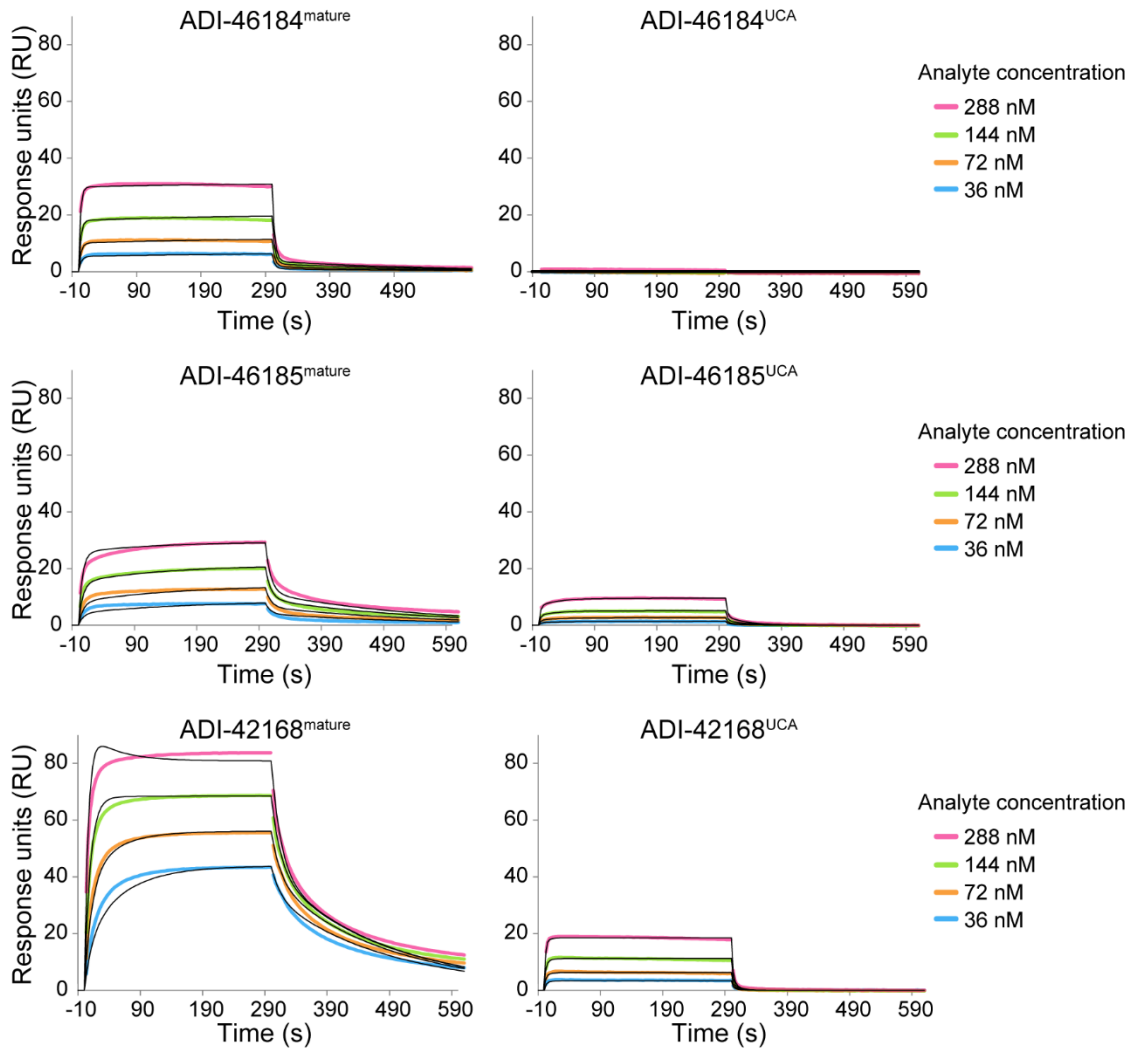
Clone name	k_{on} (1/Ms)	k_{off} (1/s)	$K_D{}^{App}$ (M)	# nucleotide substitutions
ADI-46184^{mature}	2.35E+05	2.53E-01	1.08E-06	14
ADI-46184^{UCA}	N.B.	N.B.	N.B.	0
ADI-46185^{mature}	1.04E+05	1.13E-01	1.08E-06	12
ADI-46185^{UCA}	4.58E+04	3.60E-01	7.87E-06	0
ADI-42168^{mature}	1.85E+05	5.50E-02	2.97E-07	5
ADI-42168^{UCA}	2.82E+05	4.29E-01	1.52E-06	0

Fig. S5. Binding activity of germline-reverted plasmablast mAbs. Binding traces and affinities of three somatically mutated PB-derived mAbs and their corresponding UCAs, as determined by Biacore. N.B., non-binding.
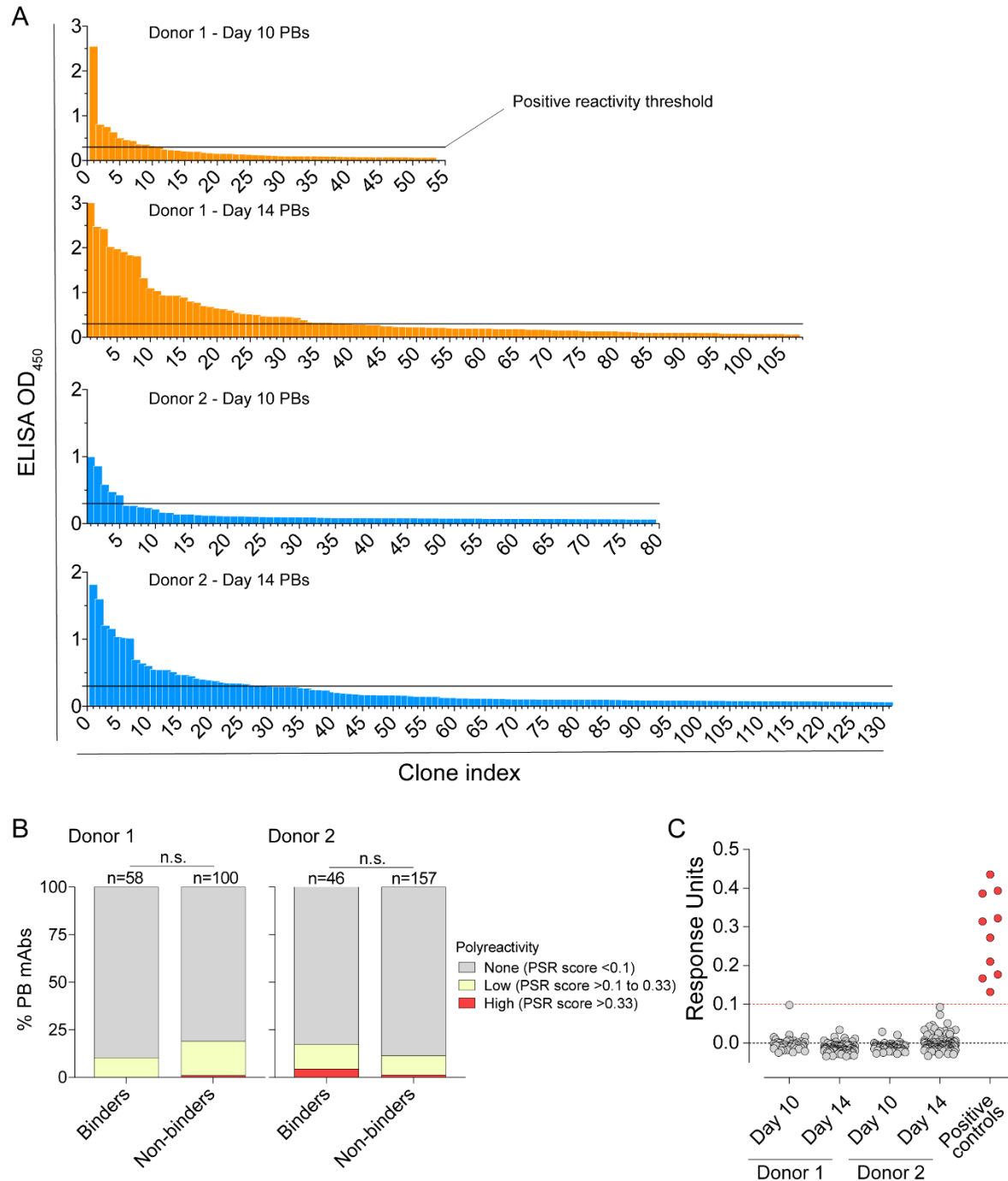
Fig. S6. Binding and polyreactivity properties of PB-derived mAbs. (A) Binding screen of PB-derived mAbs against YFV-17D viral particles immobilized by capture with murine 4G2 IgG. All mAbs were tested at a 100 nM concentration. Positive reactivity was defined as reactivity 3-fold over background. (B) Proportion of YFV-17D binding and non-binding mAbs that display high, low, or no polyreactivity, as determined using a previously described assay(9). (C) Recombinant YFV E binding reactivity of mAbs that failed to bind YFV-17D viral particles, as determined by biolayer interferometry. All mAbs were tested at a 100 nM concentration and the assay was performed in an avid orientation. Ten MBC-derived, YFV E-specific mAbs are shown as positive controls. Statistical comparisons were made using Fisher's exact test. PSR, polyspecificity reagent; n.s., not significant.
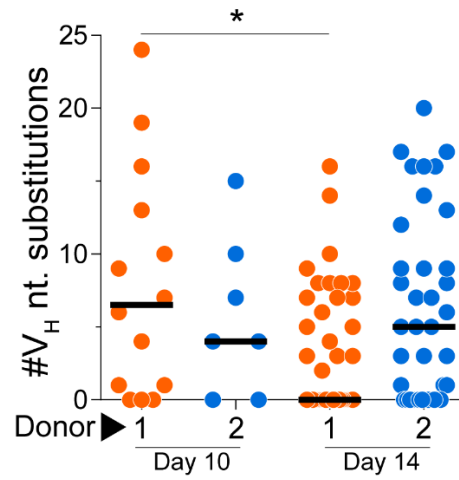
Fig. S7. SHM loads of YFV-17D binding mAbs isolated from plasmablasts. SHM loads, expressed as number of nucleotide substitutions in V_H, of YFV E-specific mAbs isolated from day 10 and day 14 PBs. PB-derived mAbs that showed binding to YFV-17D particles and/or recombinant YFV E protein were analyzed. Black bars indicate medians. Statistical comparisons were made using the Mann-Whitney test (* $P < 0.05$). nt, nucleotide; V_H, variable region of the heavy chain.
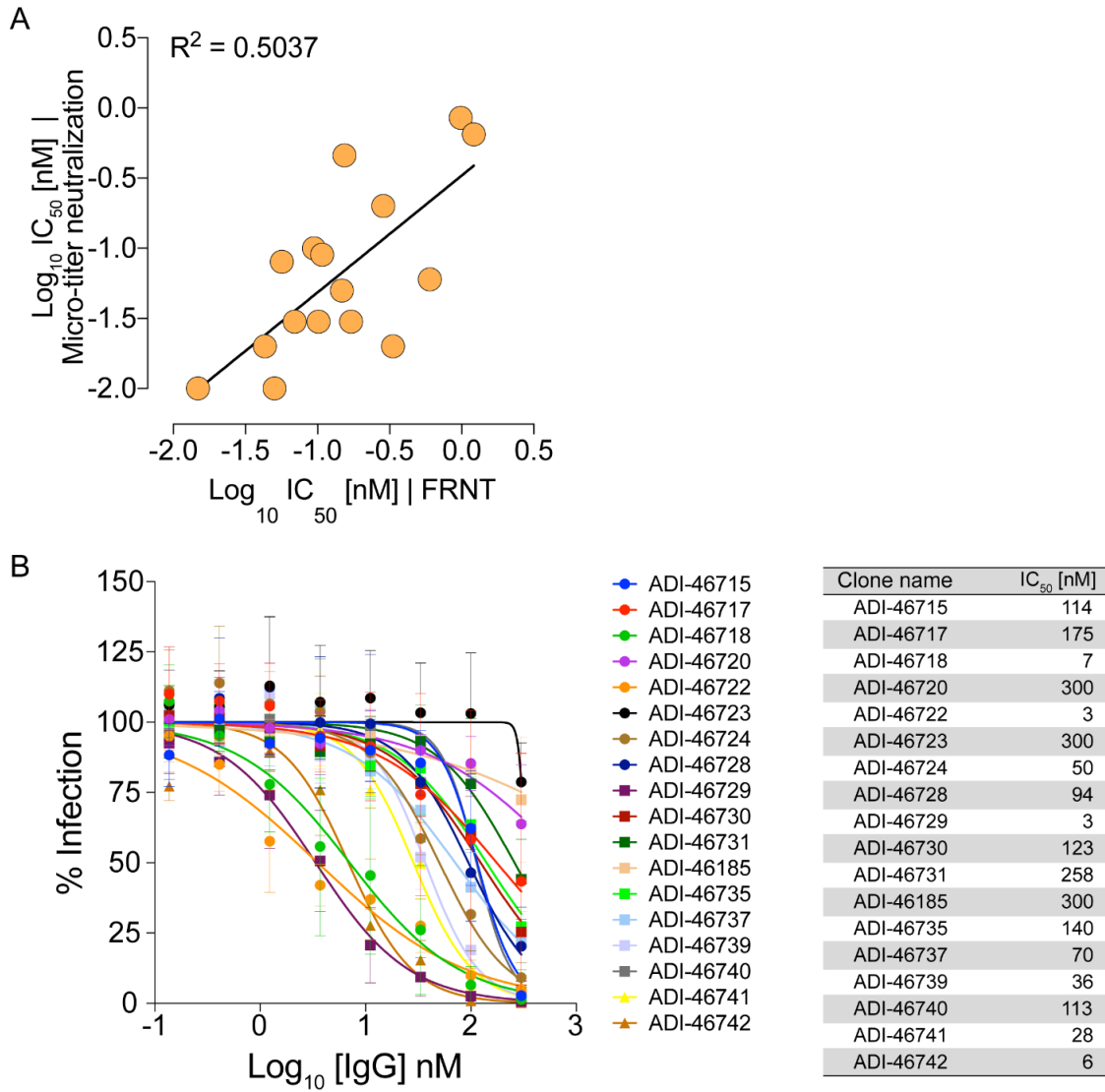
A

R² = 0.5037

B

Clone name	IC$_{50}$ [nM]
ADI-46715	114
ADI-46717	175
ADI-46718	7
ADI-46720	300
ADI-46722	3
ADI-46723	300
ADI-46724	50
ADI-46728	94
ADI-46729	3
ADI-46730	123
ADI-46731	258
ADI-46185	300
ADI-46735	140
ADI-46737	70
ADI-46739	36
ADI-46740	113
ADI-46741	28
ADI-46742	6

Fig. S8. Micro-neutralization assays. (A) A subset of mAbs isolated from donor 2 MBCs were tested for neutralizing activity in both FRNT and micro-titer neutralization assays. Neutralization IC$_{50}$s obtained in both assays are shown. R² values were generated by lineage regression analysis. **(B)** Representative YFV-17D neutralization titration curves for PB mAbs screened by micro-titer neutralization assay. Averages ± SD (n = 6) from two independent experiments are shown.

17
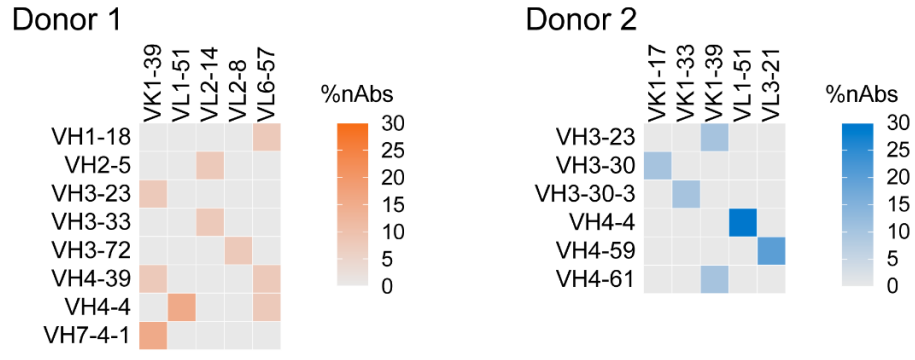
Fig. S9. V_H and V_L germline gene usage of plasmablast-derived nAbs. Heat map showing V_H and V_L germline gene usage of PB-derived mAbs that displayed neutralization IC_{50}s <100 nM against YFV-17D.
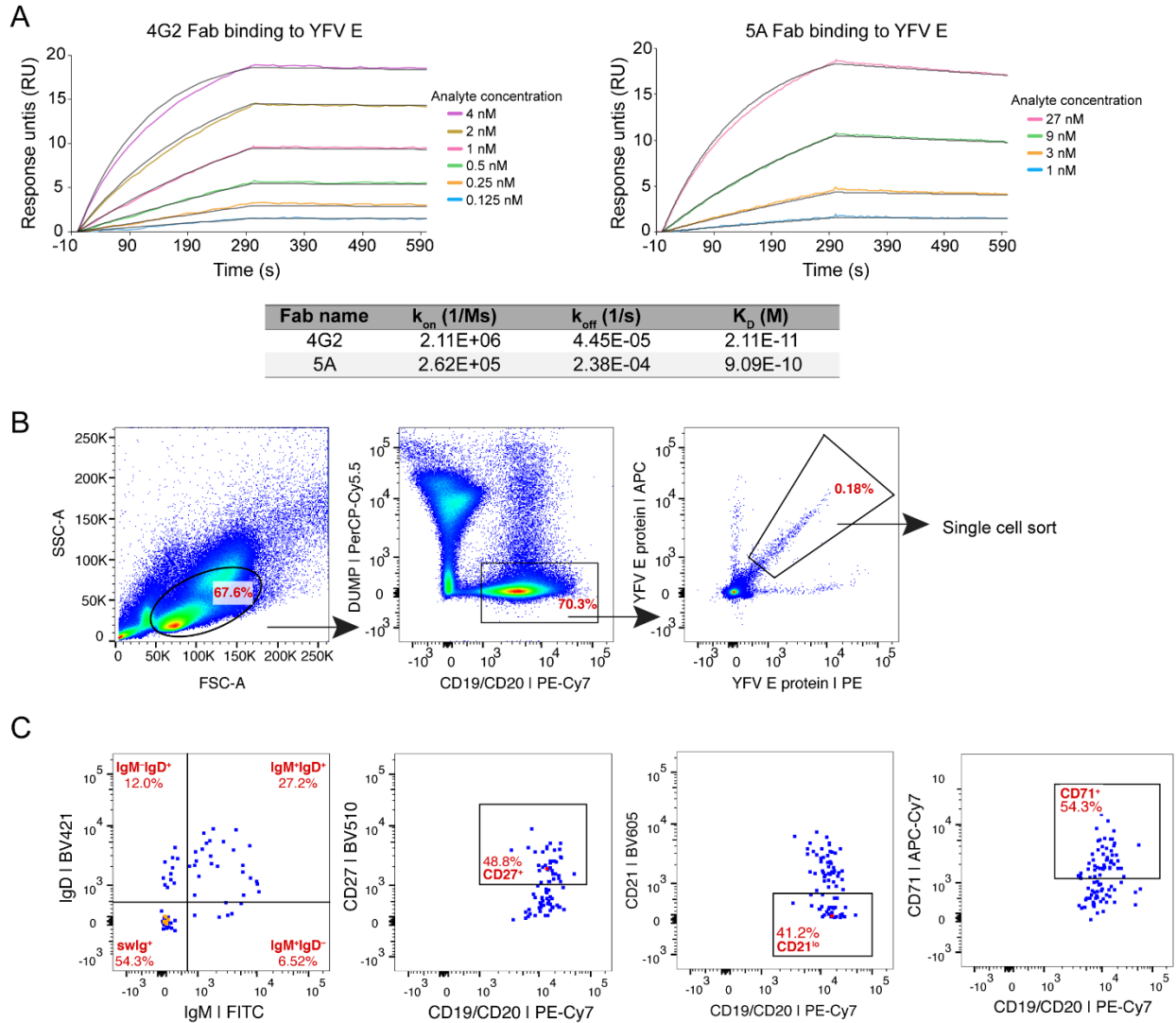
Fig. S10. Antigen quality control and YFV E-specific MBC sorting. (A) Binding of two previously described control mAbs, 4G2 and 5A, to the recombinant YFV E protein used for B cell sorting. Fab binding was assessed using Biacore. **(B)** Representative FACS gating strategy used for YFV E-specific B cell sorting. Lymphocytes were gated based on forward and side scatter, followed by selection of PI⁻ CD3⁻CD8⁻CD14⁻CD19⁺CD20⁺ cells. B cells that showed reactivity with YFV E were single-cell sorted for mAb cloning. YFV E was labeled with two different fluorophores to reduce background binding. **(C)** Representative index sort plots showing the thresholds used for defining high or low expression of the indicated surface markers. SSC-A, side scatter area; FSC-A, forward scatter area; PI, propidium iodide.
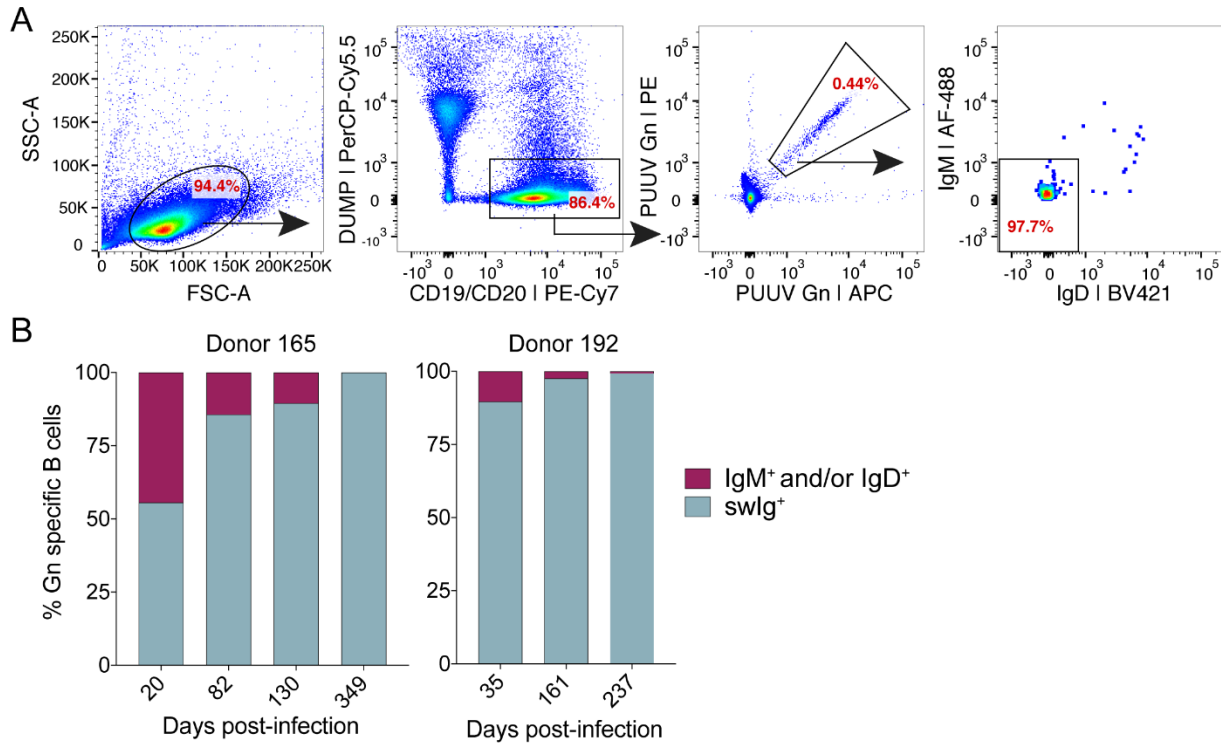
Fig. S11. Longitudinal analysis of IgM+ and swIg+ MBC responses induced by primary PUUV infection. (A) Representative FACS gating strategy used to determine IgM and IgD surface expression levels of PUUV Gn-specific B cells. The dump gate excludes cells expressing CD3, CD8, CD14, and CD16. Dead cells were also excluded by staining with propidium iodide. PUUV Gn was labeled with two different fluorophores to reduce background binding. **(B)** Percentage of PUUV Gn-specific B cells that express IgM and/or IgD or swIg on their surface, as determined by flow cytometry. SSC-A, side scatter area; FSC-A, forward scatter area.
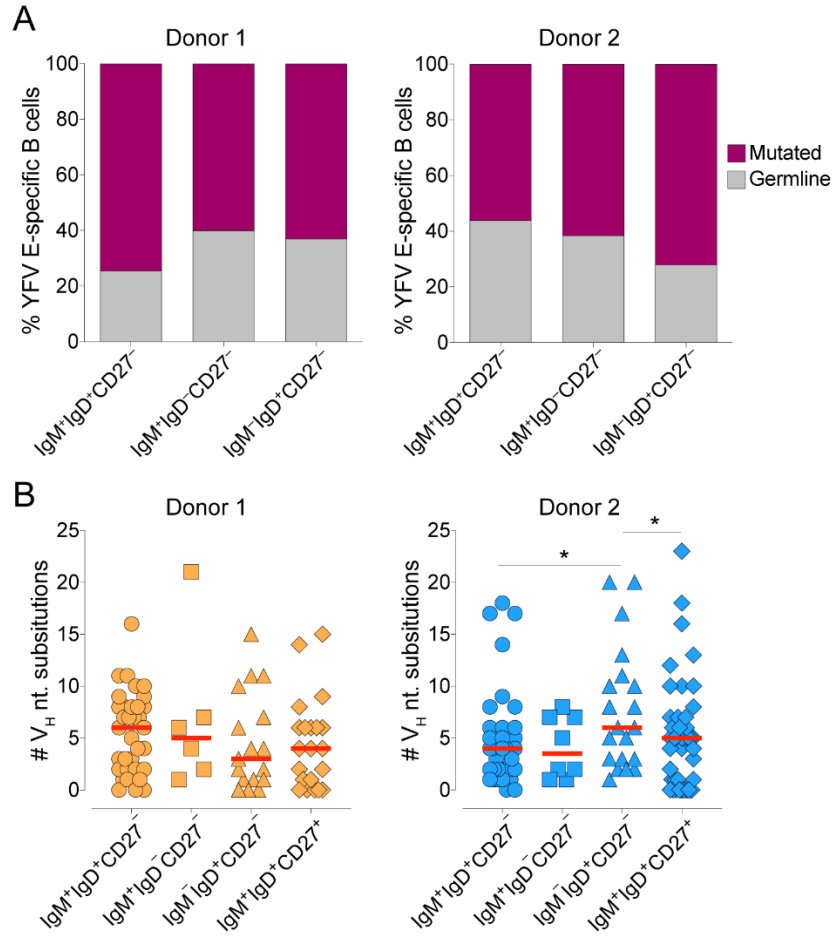
Fig. S12. Analysis of atypical MBCs induced by YFV-17D vaccination. (A) Percentage of YFV E-specific IgM+IgD+CD27−, IgM+IgD−CD27−, and IgM−IgD+CD27− B cells that contain somatic mutations. **(B)** SHM loads, expressed as number of nucleotide substitutions in V_H, of mAbs isolated from YFV E-specific IgM+IgD+CD27−, IgM+IgD−CD27−, IgM−IgD+CD27−, and IgM+IgD+CD27+ B cells. Red bars indicate medians. MAbs isolated from all time points were pooled for this analysis. Statistical comparisons were made using the Mann-Whitney test (* $P < 0.05$). Nt, nucleotide.
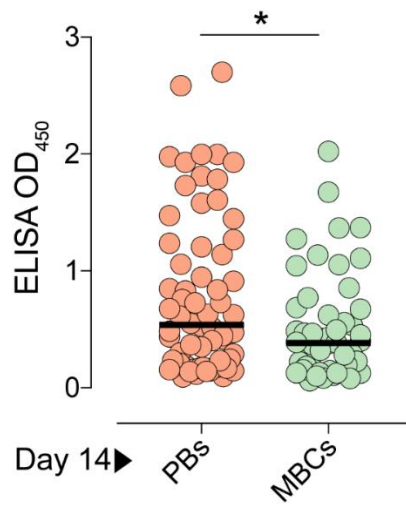
Fig. S13. YFV-17D binding activity of mAbs isolated from day 14 PBs and MBCs. ELISA binding of mAbs isolated from day 14 PBs and MBCs to YFV-17D viral particles at a 100 nM concentration. Average absorbance of two replicates is plotted. MAbs from donor 1 and 2 were combined for this analysis. Statistical comparisons were made using the Mann-Whitney test (* P < 0.05).
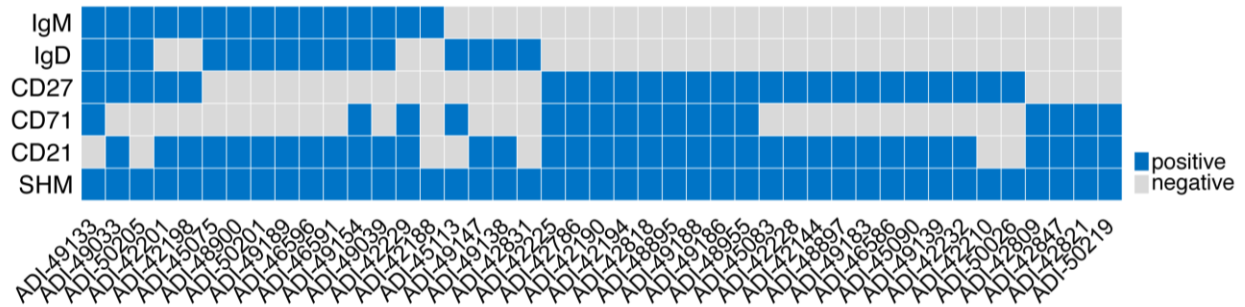
Fig. S14. Surface markers expressed on B cells from which potent nAbs were isolated. Heat map showing the presence or absence of SHM and the surface markers expressed on B cells from which highly potent (IC_{50}<1 nM) nAbs were isolated. B cell surface markers were assessed by flow cytometry.
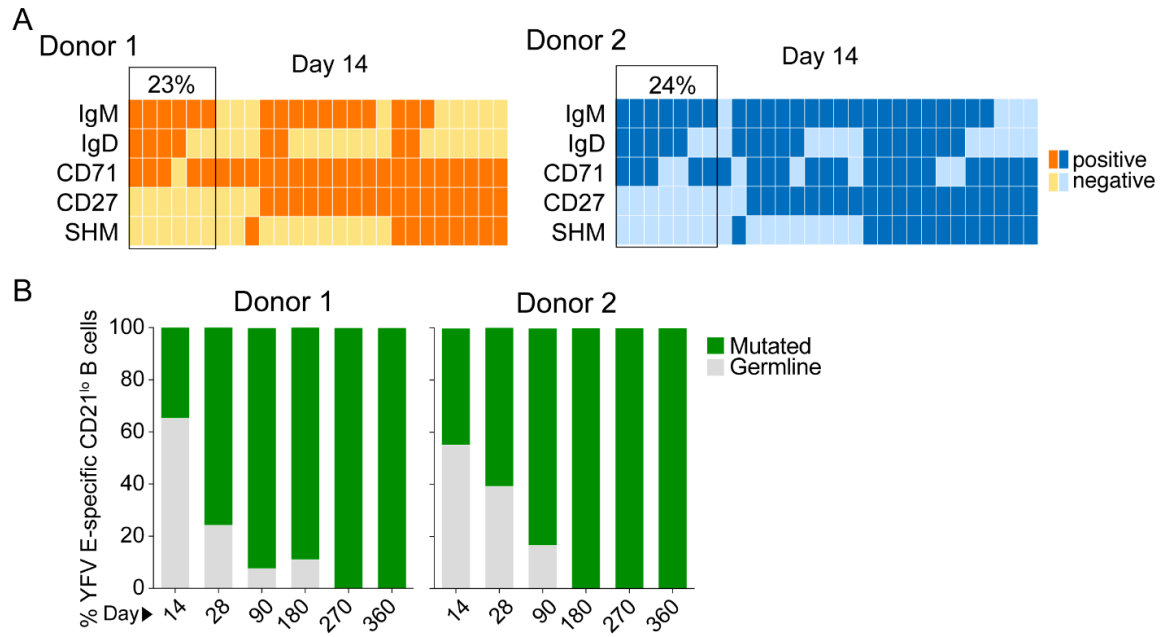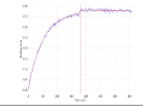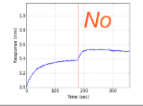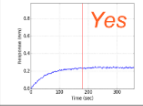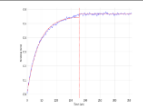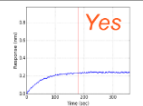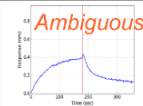
Fig. S15. Surface marker and SHM analysis of YFV E-specific CD21^{lo} B cells. (A) Heat maps show the presence or absence of SHM and the surface markers expressed on CD21^{lo} B cells from which YFV E-specific mAbs were isolated. IgM$^+$CD21^{lo}CD27$^-$SHM$^-$ B cells are indicated by boxes. B cell surface phenotypes were determined by flow cytometry. **(B)** Proportion CD21^{lo} B cells that contain somatic mutations at each sampling time point.

Antibody	Image	K_D YFV E monomer (M)	k_{on} (1/Ms)	k_{off} (1/s)	Response	Competition with 4G2	Competition with 5A
5A		9.88×10^{-10}	2.02×10^5	2.00×10^4	0.37	*No*	*Yes*
4G2		7.97×10^{-10}	2.51×10^5	2.00×10^4	0.565	*Yes*	*Ambiguous**

* Antigen dissociation from capture mAb; possible allosteric effects

Fig. S16. Cross-competition of 5A and 4G2 control mAbs. Monovalent binding affinities and cross-competition analysis of 5A and 4G2 IgGs. Binding and competition assays were performed using BLI.
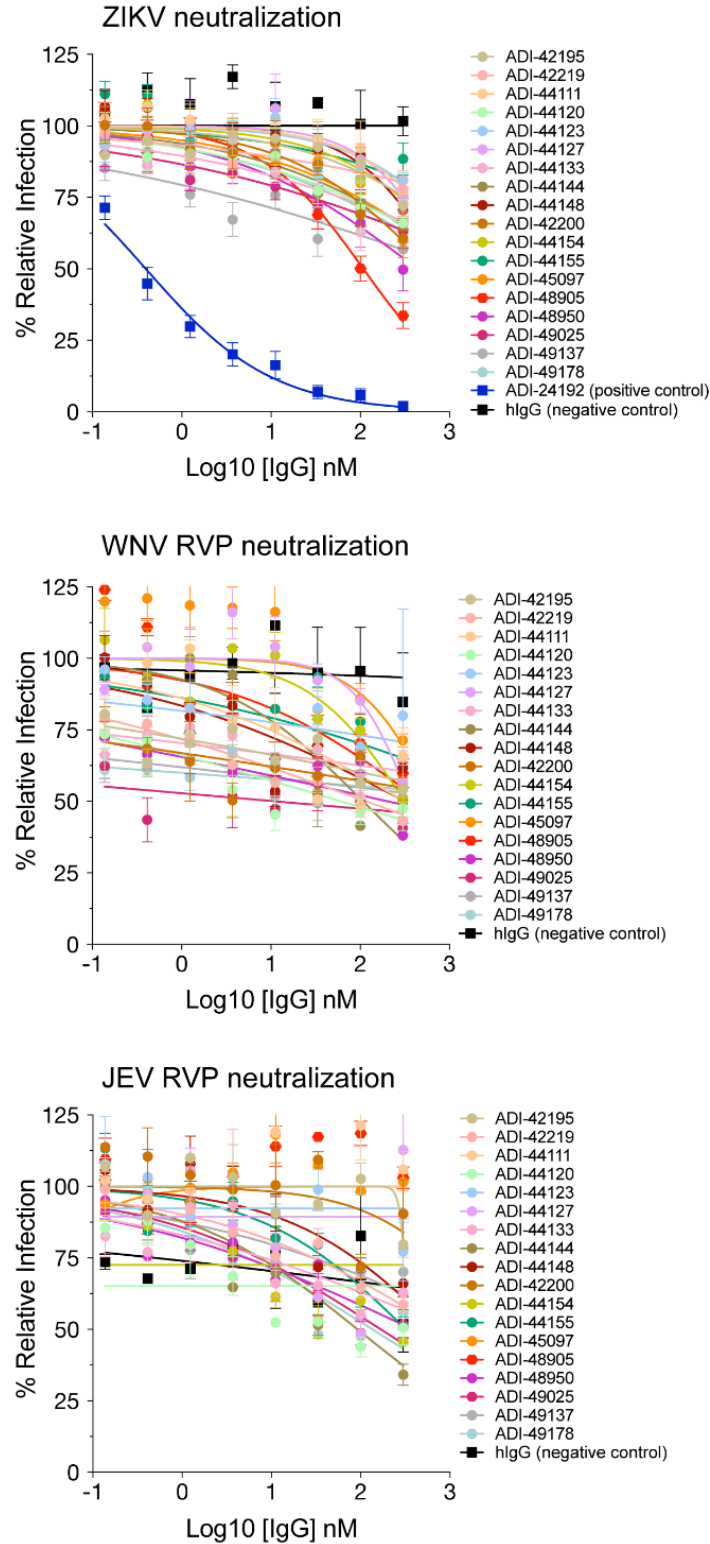
Fig. S17. Cross-neutralizing activity of mAbs displaying cross-binding activity. Cross-binding mAbs were screened for neutralizing activity against ZIKV, JEV and WNV reporter virus particles in micro-titer neutralization assay. Averages ± SD (n = 6) from two independent experiments are shown. hIgG, human purified IgG.

Table S1. Donor information.

Donor	1	2
Age	33	30
Country of origin	USA	USA
Country of residence	USA	USA
Gender	Male	Male

Table S2. Sequences and clonal lineage assignments for nAbs that compete with 5A only or both 5A and ADI-45107. MAbs utilizing VH4-4/VL1-51 germline gene pairing are highlighted in grey.

Donor	Clone name	Competition group	VH Germline	VH CDR3	VL Germline	VL CDR3	Clonal lineage number
1	ADI-46591	5A and ADI-45107	VH4-4	VRYCSSTSCYGLNGMDV	VL1-51	GTWDTRLSAL	1
1	ADI-46596	5A and ADI-45107	VH4-4	ARYCSGATCYGSNGMDV	VL1-51	GTWDFRLSAL	2
1	ADI-49188	5A and ADI-45107	VH4-4	ARDSWSGPTRNWFDP	VL1-51	GTWDSSLGGVI	3
1	ADI-46588	5A and ADI-45107	VH3-30-3	ARDAGLRIDCSSTRCLSGMDV	VK1-5	QQYNTYLLT	4
1	ADI-49186	5A	VH3-30	ARDYYASGDGYFDY	VK4-1	QQYYSTPRT	5
1	ADI-44132	5A and ADI-45107	VH3-11	ARDGSMVNAIDY	VL1-51	GTWDSSLSAAWV	6
1	ADI-46586	5A and ADI-45107	VH3-11	ARDGSMVNAIDY	VL1-51	GTWDSSLSAAWV	6
1	ADI-48955	5A and ADI-45107	VH3-11	ARDGSLVNAIDY	VL1-51	GTWDTSLSAAWV	6
1	ADI-48969	5A and ADI-45107	VH3-11	AREFSSRPFDL	VL2-11	CSYAGTYTSNYV	7
1	ADI-49183	5A and ADI-45107	VH3-11	ARELSSRIDY	VL2-14	SSYPGTSALVI	8
1	ADI-49189	5A and ADI-45107	VH3-11	AREGTRGRMD	VL2-14	SSYTSGTTLGV	9
1	ADI-49205	5A and ADI-45107	VH3-33	ARIKSDAFDL	VL2-8	FSYAGSNNYV	10
1	ADI-46001	5A and ADI-45107	VH3-11	ARDSNYFYGLDV	VL3-21	QVWDTSIDHHWV	11
2	ADI-42188	5A and ADI-45107	VH4-4	ARVVWEYSNAWCVDF	VL1-51	ETWDSSLGVVV	12
2	ADI-42198	5A and ADI-45107	VH4-4	ARVEWAYSSSWWLDY	VL1-51	GTWDTSLSAGGV	13
2	ADI-42210	5A and ADI-45107	VH4-4	ARAELSAWYYFDH	VL1-51	GTWDTSLSAGRV	14
2	ADI-42232	5A and ADI-45107	VH4-4	ARVAWTSSSSCYYDY	VL1-51	GTWDNRLSVV	15
2	ADI-42809	5A and ADI-45107	VH4-4	ARGPLKSYWYFDL	VL1-51	GTWDTSLSAGRV	16
2	ADI-49139	5A and ADI-45107	VH4-4	AKDMWAGTTTNWFGP	VL1-51	GTWDTSLGVV	17
2	ADI-49154	5A and ADI-45107	VH4-4	ARVSVSTSAWYADY	VL1-51	GTWDTSLSTV	18
2	ADI-42225	5A	VH4-4	ARIAAGYSTSWYYFDY	VL1-51	GTWDTSLSAGRV	19
2	ADI-42786	5A	VH4-4	ARDGEGHYYRSGDNWFDR	VL1-51	GTWDSSLSAVV	20
2	ADI-42818	5A	VH4-4	ARVRWSGSTSWDLDY	VL1-51	GTWDTSPSAGGV	21
2	ADI-42830	5A	VH4-4	ASTLWGGPLSVASDY	VL1-51	GTWDSSPSAGRV	22
2	ADI-45083	5A	VH4-4	ARSHWRSPQSVTFDL	VL1-51	GTWDTSSLSAGRV	23
2	ADI-49033	5A and ADI-45107	VH3-23	AKDMAVSVHRGWFDD	VK1-39	QQSYSPPMYT	24
2	ADI-49133	5A	VH3-23	AKDLAVSTPRYWFDS	VK1-39	QQSYSIPRIT	25
2	ADI-42201	5A	VH3-33	ARAQDGQQLVNYYGMDV	VK1-39	QQSYSTPYT	26
2	ADI-42821	5A	VH3-23	ARDQGFTTDWPCDY	VK1-5	QHYNSFSVK	27
2	ADI-42831	5A	VH3-23	AKDQGVTTDWPSDY	VK1-5	QHYETYSVR	28
2	ADI-42194	5A	VH4-61	AKVEEDGYTNVVRDY	VK3-11	LQRTNWPFT	29
2	ADI-42847	5A	VH4-61	VRVEEYVNNEEVRDY	VK3-11	LQRTNWPFT	30
2	ADI-45148	5A	VH3-9	AKDIGDSYGSGSYYLPYGAYYGMDV	VK3-20	QQYGSSPG	31
2	ADI-45097	5A	VH3-30	AKDSSTSWYQVVYHIDY	VL1-51	ETWDSSLNAVV	32
2	ADI-42190	5A	VH3-11	AKHTGDKPLVWAPSVYGLDV	VL2-14	SSYTRRSTLV	33
2	ADI-42849	5A and ADI-45107	VH3-11	ARDSNFNSNLDY	VL3-21	QVWDSSSDHPWV	34
2	ADI-42226	5A	VH3-72	ARVVNGLDV	VL3-25	QSADSSVADSSVV	35
2	ADI-49148	5A	VH3-72	ARVHGGGEMDI	VL3-25	QSADSRGTYVV	36

Clones highlighted in grey utilize the VH4-4 / VL1-51 germline gene combination

SI References

1. Modis Y, Ogata S, Clements D, & Harrison SC (2005) Variable surface epitopes in the crystal structure of dengue virus type 3 envelope glycoprotein. *J Virol* 79(2):1223-1231.
2. Rey FA, Heinz FX, Mandl C, Kunz C, & Harrison SC (1995) The envelope glycoprotein from tick-borne encephalitis virus at 2 A resolution. *Nature* 375(6529):291-298.
3. Modis Y, Ogata S, Clements D, & Harrison SC (2003) A ligand-binding pocket in the dengue virus envelope glycoprotein. *Proc Natl Acad Sci U S A* 100(12):6986-6991.
4. Tiller T*, et al.* (2008) Efficient generation of monoclonal antibodies from single human B cells by single cell RT-PCR and expression vector cloning. *J Immunol Methods* 329(1-2):112-124.
5. Gietz RD & Woods RA (2002) Transformation of yeast by lithium acetate/single-stranded carrier DNA/polyethylene glycol method. *Methods Enzymol* 350:87-96.
6. Bornholdt ZA*, et al.* (2016) Isolation of potent neutralizing antibodies from a survivor of the 2014 Ebola virus outbreak. *Science* 351(6277):1078-1083.
7. Abdiche YN*, et al.* (2014) High-throughput epitope binning assays on label-free array-based biosensors can yield exquisite epitope discrimination that facilitates the selection of monoclonal antibodies with functional activity. *PLoS One* 9(3):e92451.
8. Brien JD, Lazear HM, & Diamond MS (2013) Propagation, quantification, detection, and storage of West Nile virus. *Curr Protoc Microbiol* 31:15D 13 11-15D 13 18.
9. Shehata L*, et al.* (2019) Affinity Maturation Enhances Antibody Specificity but Compromises Conformational Stability. *Cell reports* 28(13):3300-3308 e3304.

Other Supporting Information Files
Dataset S1